Journal of Biomechanics 85 (2019) 141–147

Contents lists available at ScienceDirect

Journal of Biomechanics

journal homepage: www.elsevier.com/locate/jbiomech
www.JBiomech.com

Reliability of ultrasound speckle tracking with singular value decomposition for quantifying displacement in the carpal tunnel

Verena J.M.M. Schrier [a,b], Stefanie Evers [a,b], Johan G. Bosch [c], Ruud W. Selles [b,d], Peter C. Amadio [a,*]

[a] Department of Orthopedic Surgery, Mayo Clinic, Rochester, MN, United States
[b] Department of Plastic, Reconstructive and Hand Surgery, Erasmus Medical Center, Rotterdam, the Netherlands
[c] Biomedical Engineering, Thorax Center, Erasmus Medical Center, Rotterdam, the Netherlands
[d] Department of Rehabilitation Medicine, Erasmus Medical Center, Rotterdam, the Netherlands

ARTICLE INFO

Article history:
Accepted 10 January 2019

Keywords:
Speckle tracking
Singular value decomposition
Carpal tunnel
CTS
Reliability

ABSTRACT

Inhibited movement patterns of carpal tunnel structures have been found in carpal tunnel syndrome (CTS) patients. Motion analysis on ultrasound images allows us to non-invasively study the (relative) movement of carpal tunnel structures and recently a speckle tracking method using singular value decomposition (SVD) has been proposed to optimize this tracking. This study aims to assess the reliability of longitudinal speckle tracking with SVD in both healthy volunteers and patients with CTS.

Images from sixteen healthy volunteers and twenty-two CTS patients were used. Ultrasound clips of the third superficial flexor tendon and surrounding subsynovial connective tissue (SSCT) were acquired during finger flexion-extension. A custom made tracking algorithm was used for the analysis. Intra-class correlation coefficients (ICCs) were calculated using a single measure, two-way random model with absolute agreement and Bland-Altman plots were added for graphical representation.

ICC values varied between 0.73 and 0.95 in the control group and 0.66–0.98 in the CTS patients, with the majority of the results classified as good to excellent. Tendon tracking showed higher reliability values compared to the SSCT, but values between the control and CTS groups were comparable.

Speckle tracking with SVD can reliably be used to analyze longitudinal movement of anatomical structures with different sizes and compositions within the context of the carpal tunnel in both a healthy as well as a pathological state. Based on these results, this technique also holds relevant potential for areas where ultrasound based dynamic imaging requires quantification of motion.

1. Introduction

Carpal tunnel syndrome (CTS) is the most common compression neuropathy, with an estimated prevalence of 1–5% (Atroshi et al., 1999; De Krom et al., 1990). CTS is predominantly a clinical diagnosis, often supported by electrophysiological measurements. However, this is an invasive, uncomfortable method that has been criticized since it has limited negative predictive potential (Witt et al., 2004), with up to 50% of electrophysiological-negative patients still benefitting from treatment (Bland, 2001). More recently, ultrasound (US) imaging has emerged as an interesting alternative with sensitivity and specificity rates almost matching electrophysiological testing (Fowler et al., 2011). Transverse and static ultrasound parameters have been studied most extensively, with median nerve area showing the highest sensitivity rates (Nakamichi and Tachibana, 2000; Wiesler et al., 2006). However, longitudinal and dynamic assessment of the carpal tunnel structures has also gained interest. A common finding in CTS patients is non-inflammatory thickening and fibrosis of the connective tissue around the median nerve and tendon flexors (Ettema et al., 2004). The fibrotic changes in this subsynovial connective tissue (SSCT) alter the mechanical response of the tissue surrounding the median nerve to loading of the flexor tendons. Previous research has focused on measuring these patterns of (relative) motion (Filius et al., 2015b; Korstanje et al., 2012; Van Doesburg et al., 2012). Compared to non-CTS volunteers, relative median nerve motion appears inhibited, worsening with more severe symptoms (Filius et al., 2015a). Since the decision for conservative or surgical treatment is influenced by disease severity, being able to measure this non-invasively could thus aid the clinical diagnosis process and support intervention choice. However, measuring the SSCT has been challenging due to its small size.

* Corresponding author at: Tendon and Soft Tissue Biology Laboratory, Mayo Clinic, Rochester, 200 1st St. SW, Rochester, MN 55905, United States.
E-mail address: pamadio@mayo.edu (P.C. Amadio).

https://doi.org/10.1016/j.jbiomech.2019.01.022
0021-9290/

Speckle tracking is an image analysis technique that has been applied mostly to cardiac imaging (D'hooge et al., 2000) but is now also under investigation in the musculoskeletal field due to its ability to describe features of moving structures (Bohs and Trahey, 1991). Doppler imaging is similar to this technique, but is limited by its angle dependency. This method tracks the displacement of speckle patterns, the grainy texture in the ultrasound image that results from interfering ultrasound waves that are backscattered by the inhomogeneity of the tissue. Speckle tracking of tendons has been described for the Achilles tendon (Arndt et al., 2012; Bogaerts et al., 2017; Fröberg et al., 2017; Lee et al., 2008; Slane and Thelen, 2015; Stegman et al., 2014), the tibialis anterior (Gijsbertse et al., 2017), the patellar (Slane et al., 2018), the flexor digitorum superficialis (FDS) (Korstanje et al., 2010; Stegman et al., 2014; van Beek et al., 2018) but also for the median nerve (Dilley et al., 2001; Filius et al., 2015a).

Relative SSCT motion has been assessed using commercial tracking software in both healthy volunteers (Yoshii et al., 2009) as well as in patients with CTS (Van Doesburg et al., 2012), but this type of tracking is limited because the software limits the settings that the user can change manually in order to optimize the tracking on individual patient basis.

Recently, a custom made speckle tracking algorithm was extended with a background suppression technique based on Singular Value Decomposition (SVD) (Demené et al., 2015) in order to minimize the effect of clutter and noise of stationary background. This improved approach could provide a cleaner look at the differential movement of the FDS and how the relationship between the SSCT and neighboring structures changes in CTS. Since ultrasound imaging and speckle tracking are both subjected to operator interpretation, variability in image acquisition and analysis needs to be assessed. If reliability can be established, it also provides interesting potential applications in the image processing of any musculoskeletal assessment where dynamics and biomechanics play a role. Therefore, using the context of the carpal tunnel structures, this study evaluates three aspects of reliability of speckle tracking with SVD: (1) intra-rater, reflecting the variation in measurements done by a single rater, (2) inter-rater analysis, reflecting the variation between two raters who measure the same subjects (Koo and Li, 2016), and (3) repeatability (also referred to as test-retest reliability), reflecting the variation in measurements acquired at multiple time points.

2. Methods

2.1. Data collection

Ultrasound images were obtained from a sample of patients with CTS and from volunteers without CTS, referred to as control group. The Mayo Clinic Institutional Review Board approved both studies (control group IRB#06-002950, patients with CTS IRB#14-003444). Written consent was obtained from all participants.

2.1.1. Control group

Seventeen subjects between the ages of 18–85 years were included. Exclusion criteria were: history of CTS, rheumatoid arthritis, osteoarthritis or traumatic injuries of the ipsilateral hand or wrist. All imaging was done according to a preset imaging protocol described below.

2.1.2. Patients with CTS

A dataset was constructed by randomly selecting twenty-two patients included in a prospective randomized controlled trial (ClinicalTrials.gov, identifier: NCT02219555). Patients were recruited after being diagnosed with CTS in a hand clinic by any of the hand physicians. Diagnoses were made based on clinical presentation and EMG results as described in the guideline from the American Academy of Orthopaedic Surgeons (AAOS, 2016). Inclusion criteria were clinical diagnosis of CTS, age between 21 and 80 years, symptoms of numbness or tingling for at least 4 weeks, and indication for treatment with injection or surgical release. Exclusion criteria were a previous surgical release, tumor, deformity in hand/wrist, previous history of steroid injection, and any known risk factor for non-idiopathic CTS (including pregnancy, diabetes, rheumatoid arthritis). Clinical evaluations included two point discrimination, Phalen's test, Tinel's sign, manual muscle testing of the abductor pollicis brevis, and notation of the presence of thenar muscle atrophy.

2.2. Imaging protocol

Ultrasound recordings were collected from the patients prior to their treatment. Each subject was imaged in supine position on a bed with the elbow (of the affected hand in CTS cases) fully extended, the shoulder in abduction (70–80 degrees) and the forearm supinated stretched out on an acrylic glass board. One strap was used to minimize forearm movement and another to inhibit overextension of the third digit and flexion of the second and fourth digit. An ultrasound scanner Philips iE33 (Royal Philips Electronics, Amsterdam, the Netherlands) equipped with 15L7 linear array transducer was used. The transducer was placed at the wrist in a sagittal plane over the proximal wrist crease with the wrist in the neutral position. If necessary, a folded pillowcase was placed under the hand to straighten the wrist. The transducer was applied to the skin without additional pressure and with plenty of gel. Participants were asked to flex and extend the third digit corresponding to a frequency of fifty beats per minute under guidance of a metronome (Fig. 1, Suppl video 1). After a practice round, three ultrasound clips with each three flexion-extension cycles were recorded. All images were taken following the same ultrasound protocol, with the same machine by two different ultrasonographers (VS & SE) who were both trained in using the protocol.

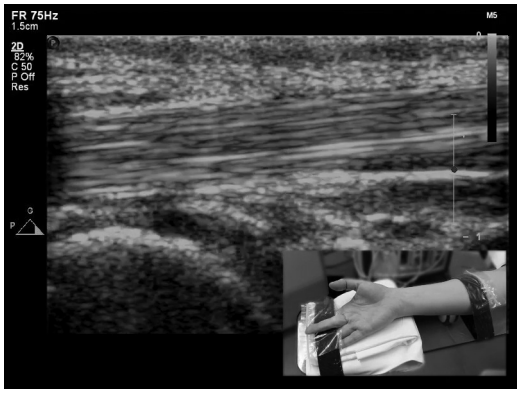

Video 1. Synchronized ultrasound recording with participant flexing and extending the third digit to illustrate the relation between the movement and the image.

2.3. Data analysis

After image acquisition, all images were analyzed using a Matlab based custom made algorithm developed at the Erasmus MC for speckle tracking with singular value decomposition which had already been tested in an animal model and validated for tendon tracking (Bandaru et al., 2018; Korstanje et al., 2010). Before setting the region of interest (ROI), the complete clip was reviewed

Fig. 1. Example of start (left) and end (right) position of the third digit during the flexion-extension cycle. Each recording contained three cycles.

to identify the median nerve, the SSCT, the FDS and the flexor digitorum profundus (FDP). Then, image analysis took place in three stages (Fig. 2). First, the ROI was manually placed with its proximal border at the level of the radial head, covering the width of the tendon, but without incorporating movement of the adjacent FDP. The ROI was fixed during motion with a pre-set 1:4 size ratio, and could be rotated to ensure a position parallel to the tendon fibrils. Immediately after placement, a feedback video would play with the ROI added for the analyst to review whether it correctly captured the desired structure throughout the entire clip (Fig. 3). In some cases, the tendon would show apparent movement in the volar-dorsal plane in which case, if possible, the ROI would be adjusted in size. Differences in ROI box sizes were negligible, since tendon widths were comparable. In cases where additional kernel size and number fine tuning were deemed necessary, images were excluded. For the SSCT, a similar method was used, but with a separate ROI covering the visible SSCT. The position of the ROI was placed directly volar to the tendon ROI to measure relative motion. The SSCT's organization shows multiple horizontal sheets (Ettema et al., 2004) and to account for different speeds at different levels,

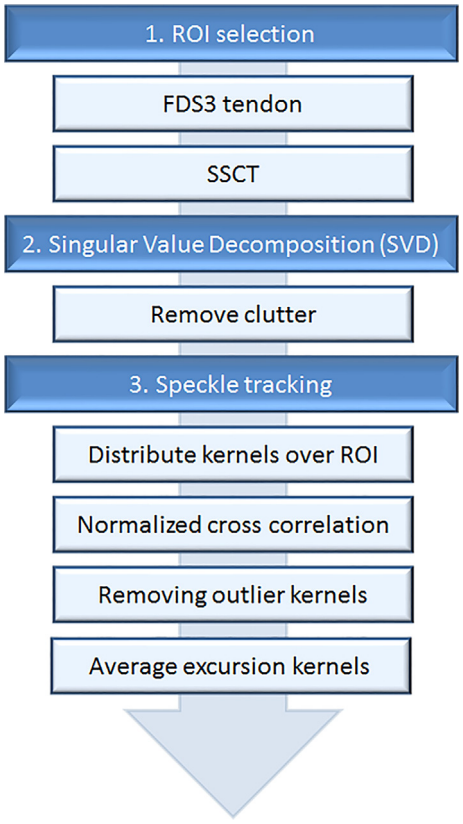

Fig. 2. General overview of the image analysis sequence including the singular value decomposition.

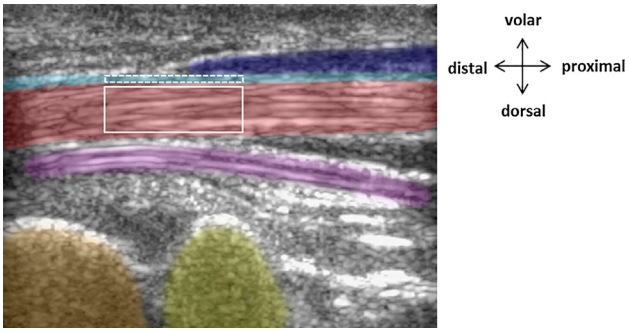

Fig. 3. Ultrasound B-mode image with color overlay to indicate the anatomical structures in a sagittal plane. From volar to dorsal, dark blue: median nerve, light blue: SSCT between tendon and median nerve, red: FDS3, purple: FDP 3, orange: lunate, yellow: radius. The box with the solid demarcation depicts an example of a ROI over the entire width of the superficial tendon. The box with the interrupted line shows the ROI for the SSCT. (For interpretation of the references to color in this figure legend, the reader is referred to the web version of this article.)

the analysis was performed over five evenly-spaced vertical layers within the SSCT ROI. After placing both ROIs, a temporary video file was created that was used as input for the speckle tracking. The algorithm has been described in detail before (Bandaru et al., 2018), but in short, consists of first the SVD filtering followed by the speckle tracking. The SVD filter is an improvement on the more classically used high-pass clutter filter; It decomposes the sequence into specific motion components, which allows noise (incoherent-high frequency signals) as well as clutter removal (high intensity-low frequency), minimizing the signal of static and slow moving structures in the image sequence. Then, within the ROI, a set of overlapping 2D kernels was defined and block matching with normalized cross correlation was applied for each of them to find the frame-to-frame displacement vector. Finally, as described by Bandaru et al. (Bandaru et al., 2018), unreliable kernel results were removed based on their correlation values and discordant vectors. The average of the displacement vectors of the reliable kernels gave the final frame-to-frame displacement vector.

The analyses were done using Matlab (R2016a, The MathWorks Inc., Natick, MA, 2000). The Euclidean length of the total displacement vector was calculated in mm. The input used for reliability analyses were the excursion and shear index over 3 cycles (equal to six movements). The shear index is a measure for relative motion between the third FDS and SSCT and was defined as:

$$Shear\ \ index = \frac{Tendon\ \ Excursion - SSCT\ \ excursion}{Tendon\ \ Excursion} * 100\%$$

An index value of 0% indicates that the SSCT moved in equal amount with the tendon whereas 100% would indicate a complete dissociation. All analyses were done in random order and the rater who performed the analyses was blinded to the results of their previous assessment and the results of the other rater.

Table 1
Summary of absolute displacement results and shear indices in both groups. Means were calculated based on measurements over three consecutive flexion-extension cycles derived from the first data set from one of the raters. FDS: Flexor digitorum superficialis, SSCT: Subsynovial connective tissue, Shear index: ratio of the difference in motion between FDS and SSCT over the total motion of the FDS.

	Control group	CTS patients
Number of participants	16	22
FDS displacement in cm; Mean (SD)	6.8 (2.4)	8.4 (2.5)
SSCT displacement in cm; Mean (SD)	1.5 (0.7)	2.1 (0.8)
Shear index in %; Mean (SD)	78 (9.7)	73 (13.2)

Three aspects of reliability were analyzed:

Intra-rater reliability: For measurement of the main rater-dependable factor of the speckle tracking (placement of region of interest), the recordings from both groups were analyzed in random order twice by the same rater with a time interval of three-four weeks. The first set of results was also used for the inter-rater reliability and the repeatability. *Inter-rater reliability*: In order to measure the variance between different raters, a second analyst measured the same set of clips derived from both the control group and the CTS patients. *Repeatability*: Repeatability was defined as the variation in measurements derived from the same subject, under equal circumstances, directly after an initial clip was recorded. Any differences measured therefor must be the summation of the variance in the recording and the analysis.

2.4. Statistical analyses

To quantify reliability, intra-class correlation coefficients (ICCs) including the 95% confidence interval were calculated, using a two way random effects model with single measure and absolute agreement. In general, ICC values above 0.75 are considered as excellent, values between 0.40 and 0.74 are fair to good and values below 0.40 are considered as poor, in accordance with the classification proposed by Fleiss (Fleiss, 2011). Agreement was evaluated using Bland Altman plots with 95% limits of agreement (Bland and Altman, 1986). Distribution of the difference of means was tested for normality visually with histograms and normal quantile plots and statistically with the Shapiro-Wilk test of normality (Shapiro and Wilk, 1965). In case of normality, the plots were made with limits of agreement as calculated by the mean difference ± 1.96 × SD of the difference. In case of non-normal distribution, a logarithmic transformation of the data was performed after which the same calculation for the limits was done (Bland and Altman, 1999). Statistics were done using IBM Statistical Package for Social Sciences software version 22 (SPSS, Chicago, IL, USA).

3. Results

In total, images from seventeen healthy volunteers and twenty-two CTS patients were analyzed. The clips of one control participant were labeled as too low image quality to include since the tendon and SSCT moved significantly in volar-dorsal direction and out of plane, causing the structures of interest to fall out of the ROI. After exclusion, the remaining sixteen healthy volunteer clips were used for analyses.

The absolute values for the tendon, SSCT and shear index are summarized in Table 1. The shear indices are arguably the parameter of most interest since it is the disturbance of the relative motion due to fibrosis of the SSCT that would underlie the hypothesized pathophysiology of idiopathic CTS. The shear index values found in the control versus the CTS group ranged between 56% and 90% with an average of 78% versus 41%–93% with an average of 73% respectively.

The intra-rater, inter-rater and repeatability ICCs of the tendon and SSCT are shown in Table 2. All tendon ICC values can be classified as excellent, as well as the majority of the SSCT comparisons. Only SSCT inter-rater and repeatability in the CTS patients classified as good with 0.70 and 0.74 respectively. In the control group, values for the shear indices ranged between good and excellent (intra-rater: 0.87, inter-rater: 0.74, repeatability: 0.73). This was also found in the CTS group except for a lower ICC value of 0.66 for the inter-rater reliability. Bland Altman plots for the intra-, inter-rater and repeatability reliabilities of the shear index are shown in Fig. 4A–F. By plotting the average between two measurements against the difference between those measurements, any funnel-like shapes would indicate a more profound disagreement with either a decrease or increase in the average value. Only in the inter-rater comparisons and the repeatability of the CTS group (Fig. 4C, D & F) can a slight tendency of more disagreement be found with lower values. However, most values still fall within the 95% confidence limits.

4. Discussion

This study assessed the reliability of a speckle tracking algorithm with singular value decomposition to track absolute and relative motion of longitudinal structures inside the carpal tunnel. Based on our sample of both CTS and non-CTS subjects, we found mostly good to excellent reliability. The lowest ICC value, for the inter-rater comparison of the shear index, can still be classified as moderate to good.

Although several publications describe speckle tracking for analysis of carpal tunnel structures, not many have described reliability. Filius et al. have used a similar speckle tracking analysis without SVD and published test-retest values for both the third FDS tendon and its superficial layer of SSCT. They note ICC values of 0.70 and 0.73 respectively (Filius et al., 2015a). Their repeatability measurements were done in a larger group (n = 50) and reliability data was from both healthy and CTS patents combined. Using Doppler imaging, FDP excursion reproducibility was assessed in both a healthy group (Soeters et al., 2004a) as well as a patient group with tendon injury (Soeters et al., 2004b). They presented

Table 2
Reliability of structure displacement measurements including relative motion (shear index) for both the control and the CTS group. ICC's were calculated using two way random model with absolute agreement and include the 95% confidence intervals. Control group n = 16, CTS patient group n = 22. FDS: Flexor digitorum superficialis, SSCT: Subsynovial connective tissue, CI: Confidence interval, Shear index: ratio of the difference in motion between FDS and SSCT over the total motion of the FDS.

	Control group						CTS patients					
	FDS		SSCT		Shear index		FDS		SSCT		Shear index	
	ICC	95% CI	ICC	95% CI	ICC	95% CI	ICC	95% CI	ICC	95% CI	ICC	95% CI
Intra-rater	0.94	0.84–0.98	0.93	0.82–0.98	0.87	0.66–0.95	0.98	0.95–0.99	0.81	0.59–0.92	0.82	0.61–0.92
Inter-rater	0.95	0.86–0.98	0.82	0.56–0.93	0.74	0.41–0.90	0.82	0.59–0.92	0.70	0.38–0.87	0.66	0.32–0.85
Repeatability	0.89	0.72–0.96	0.82	0.55–0.93	0.73	0.40–0.90	0.88	0.74–0.95	0.74	0.47–0.88	0.82	0.61–0.92

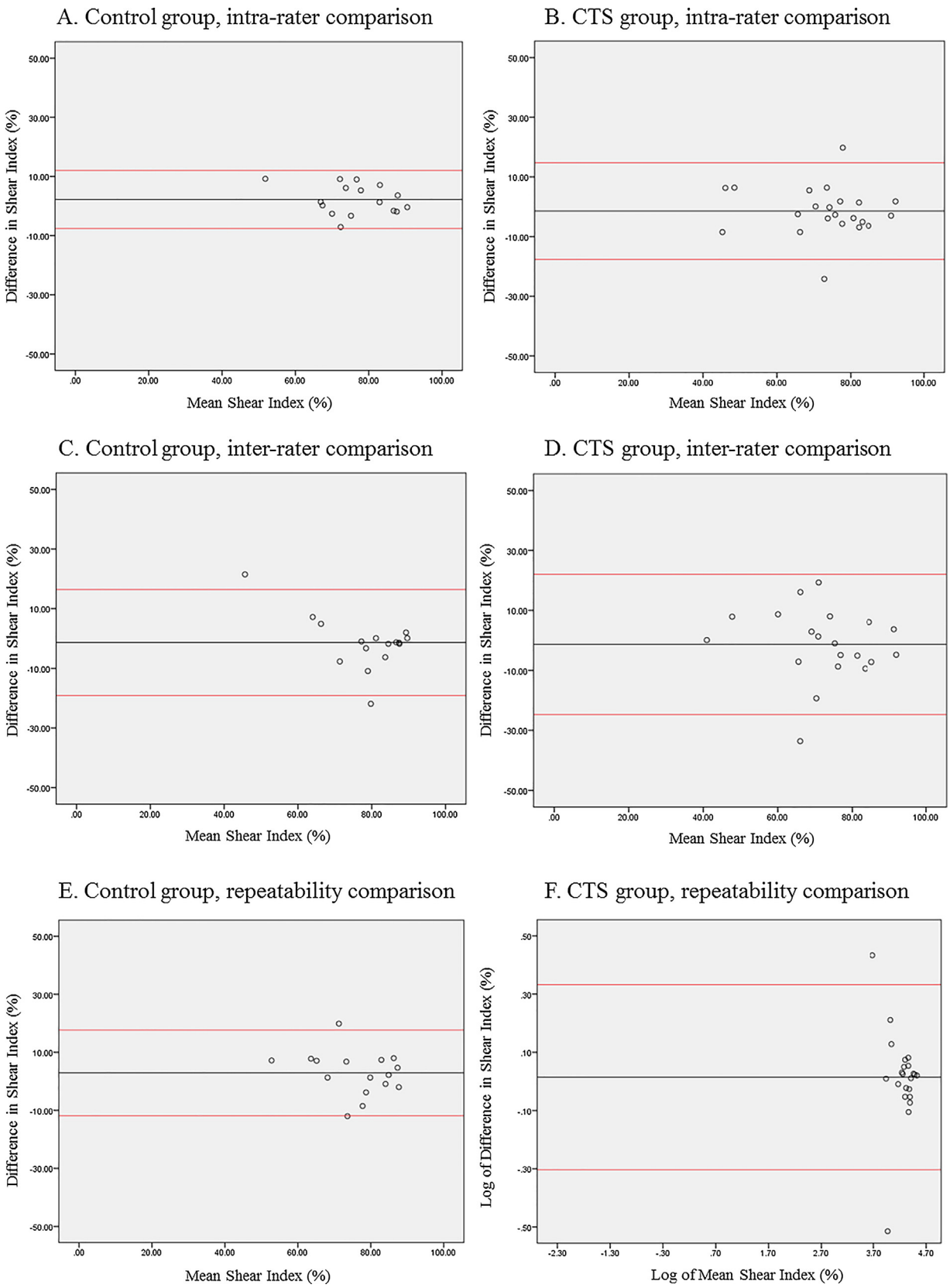

Fig. 4. A–F: Bland Altman plots showing the intra- (A and B), inter-rater (C and D) and the repeatability (E and F) data of the shear index for both tested groups. These plots have the mean of two measurements on the x-axis plotted against the difference between the two values. The black line and red lines indicate the average difference and the 95% upper and lower limit respectively for the compared samples. Data for figure F was logarithmically transformed due to the non-normal distribution of the data. (For interpretation of the references to color in this figure legend, the reader is referred to the web version of this article.)

ICC values of 0.81 and 0.88 respectively at ten days post intervention. Despite the difference in imaging depth, their results are similar to ours.

In general, our SSCT ICC values tended to be lower than those for the tendon which was also the case in similar research (Filius et al., 2015a). This can in part be explained by the anatomical differences; The FDS tendon has a width of about ten times the SSCT (<1 mm) and thus can accommodate a larger ROI which is less susceptible to movement in the volar-dorsal plane. In addition, the SSCT is a layered structure, so during tracking the displacement can differ based on the position. This should receive extra consideration when imaging patients with CTS, because higher levels of fibrosis have been found to occur in the layers closest to the tendon (Ettema et al., 2006).

In this study, an average of 1.1 cm (control group) and 1.4 cm (CTS group) excursion of the tendon was found per flexion/extension movement (data shown in the results is total over three cycles with two movements each), which is comparable to what colleagues have found; Korstanje et al. used a similar algorithm, without SVD, on CTS patient-derived clips and found a mean tendon excursion of 1.98 cm but do not report any ICC values (Korstanje et al., 2012). Filius et al. published two studies with CTS patients (Filius et al., 2015a; Filius et al., 2015b) where they used the same algorithm without SVD, and found average tendon excursions of 1.88 cm and 1.44 cm (calculated based on published values). Control data showed 1.56 cm and 1.43 cm FDS3 excursion. To test whether the difference in tendon excursion in the present study could be due to anthropometric differences between the groups, post hoc hand measurements from the distal wrist crease to the tip of the long finger were made. This indeed showed a small but significant size difference (CTS: 20.3 ± 1.8 cm, controls: 18.7 ± 1.0 cm). However, the quality of the CTS patient pictures was suboptimal, leading to less accurate measurements. Perhaps more importantly, we do not have data on the individual amount of finger flexion during the trials. Someone with a large hand could still have a small tendon excursion if their maximum finger flexion was smaller. Although there is evidence that hand morphology is associated with CTS, it seems to be the ratio between wrist width and depth that differs most between controls and CTS patients (Farmer and Davis, 2008). So far, this seems to hold limited diagnostic and prognostic value (Mondelli et al., 2015).

Excursion values for SSCT were published in two articles, 1.55 cm and 0.74 cm for CTS groups and 1.30 cm and 0.76 cm in control groups (Filius et al., 2015a; Korstanje et al., 2012). Although Korstanje found a significant difference in SSCT excursion between the most and least affected hand ($p = 0.025$), this was not found in the study by Filius et al. and explained by possible greater inter-subject variability. Our study found an average of ~0.3 cm SSCT excursion in both the patients with CTS as the healthy group, but all results are susceptible to noticeable standard deviations. Additionally, our study was not primarily designed for absolute value comparison and our absolute values represent the total excursion over three cycles. Previously, a validation of the speckle tracking (Bandaru et al., 2018) was done for tendons and ideally the same would be done for the SSCT. However, this is challenging, even with a phantom or cadaver model, due to the small size of the SSCT and the likelihood of disrupting the complex microstructure with markers.

Strengths of this study are that we tested an innovative technique to measure ultrasonically captured motion of small anatomical structures, expanding the boundaries of what speckle tracking can detect and be utilized for. Insights gained into the limitations of speckle tracking can help contextualize results whether acquired for research or clinical purposes. In addition, utilizing dynamic features and interrelations of the carpal tunnel structures to support CTS therapy choice is a novel approach. Limitations of the study include that speckle tracking inherently does not take out of plane motion into account, which may result in underestimation of the actual motion. We also used a high frequency probe to allow visualization of the SSCT, which might have supported the high ICC values. Additionally, it was reported that the tracking depends on the balance between tendon velocity and acquired frame rate, with a decrease in validity if these parameters fall outside of predetermined boundaries (Bandaru et al., 2018). In our situation this was, prevented by adding a metronome during acquisition, but this does not eliminate the variation in the participant's cooperation and ability to perform a repeatable movement. If, in a clinical application baseline images are compared to a follow-up, changes in finger movement should be taken into account via either a rigid acquisition protocol or an outcome measure insensitive to total excursion (like shear index). Additionally, the ICC values presented in this study do indicate that future data on shear index in the carpal tunnel should be re-evaluated within different contexts. For example, for a study-based purpose, a single rater would be fine, but for clinical application, more research including multiple raters would be needed.

In conclusion, this study shows that SVD enhanced speckle tracking can reliably be used to analyze (relative) longitudinal SSCT displacement both in participants with and without CTS. Together with the validation data, our results imply that dynamic ultrasonic measurements of carpal tunnel structures can be used to further explore the potential of using this technique to help guide and predict CTS treatment outcomes. Although our study focuses on CTS related anatomical structures, the principles of the image analysis could be extrapolated to other research areas involving pathologies where the assessment of dynamic imaging is of relevance.

Acknowledgement

The authors would like to thank Raja Bandaru for his technical assistance during the experimental phase of the study.

Conflict of interest statement

None of the authors have any commercial associations that might pose or create a conflict of interest with information presented in the submitted manuscript. None of the authors received payments or other benefits or a commitment or agreement to provide such benefits from a commercial entity. Data presented in this manuscript has been presented on poster at the Orthopedic Research Society conference, New Orleans, Louisiana in 2018.

References

AAOS, 2016. American Academy of Orthopaedic Surgeons, Management of carpal tunnel syndrome evidence-based clinical practice guideline. Avalaible at: www.aaos.org/ctsguideline.

Arndt, A., Bengtsson, A.-S., Peolsson, M., Thorstensson, A., Movin, T., 2012. Non-uniform displacement within the Achilles tendon during passive ankle joint motion. Knee Surg. Sports Traumatol. Arthrosc. 20 (9), 1868–1874.

Atroshi, I., Gummesson, C., Johnsson, R., Ornstein, E., Ranstam, J., Rosén, I., 1999. Prevalence of carpal tunnel syndrome in a general population. JAMA 282 (2), 153–158.

Bandaru, R.S., Evers, S., Selles, R.W., Thoreson, A.R., Amadio, P.C., Hovius, S.E., Bosch, J.G., 2018. Speckle tracking of tendon displacement in the carpal tunnel: improved quantification using singular value decomposition. IEEE J. Biomed. Health. Inf., advanced online publication. https://doi.org/10.1109/JBHI.2018.2822548.

Bland, J.D., 2001. Do nerve conduction studies predict the outcome of carpal tunnel decompression? Muscle Nerve: Off. J. Am. Assoc. Electrodiag. Med. 24 (7), 935–940.

Bland, J.M., Altman, D., 1986. Statistical methods for assessing agreement between two methods of clinical measurement. Lancet 327 (8476), 307–310.

Bland, J.M., Altman, D.G., 1999. Measuring agreement in method comparison studies. Stat. Methods Med. Res. 8 (2), 135–160.

Bogaerts, S., Carvalho, C.D.B., Scheys, L., Desloovere, K., D'hooge, J., Maes, F., Peers, K., 2017. Evaluation of tissue displacement and regional strain in the Achilles

tendon using quantitative high-frequency ultrasound. PloS one 12 (7), e0181364.
Bohs, L.N., Trahey, G.E., 1991. A novel method for angle independent ultrasonic imaging of blood flow and tissue motion. IEEE Trans. Biomed. Eng. 38 (3), 280–286.
D'hooge, J., Heimdal, A., Jamal, F., Kukulski, T., Bijnens, B., Rademakers, F., Sutherland, G., 2000. Regional strain and strain rate measurements by cardiac ultrasound: principles, implementation and limitations. Eur. J. Echocardiogr. 1 (3), 154–170.
De Krom, M., Kester, A., Knipschild, P., Spaans, F., 1990. Risk factors for carpal tunnel syndrome. Am. J. Epidemiol. 132 (6), 1102–1110.
Demené, C., Deffieux, T., Pernot, M., Osmanski, B.-F., Biran, V., Gennisson, J.-L., Correas, J.-M., 2015. Spatiotemporal clutter filtering of ultrafast ultrasound data highly increases Doppler and Ultrasound sensitivity. IEEE Trans. Med. Imaging 34 (11), 2271–2285.
Dilley, A., Greening, J., Lynn, B., Leary, R., Morris, V., 2001. The use of cross-correlation analysis between high-frequency ultrasound images to measure longitudinal median nerve movement. Ultrasound Med. Biol. 27 (9), 1211–1218.
Ettema, A.M., Amadio, P.C., Zhao, C., Wold, L.E., An, K.-N., 2004. A histological and immunohistochemical study of the subsynovial connective tissue in idiopathic carpal tunnel syndrome. JBJS 86 (7), 1458–1466.
Ettema, A.M., Amadio, P.C., Zhao, C., Wold, L.E., O'byrne, M.M., Moran, S.L., An, K.-N., 2006. Changes in the functional structure of the tenosynovium in idiopathic carpal tunnel syndrome: a scanning electron microscope study. Plast. Reconstr. Surg. 118 (6), 1413–1422.
Farmer, J., Davis, T., 2008. Carpal tunnel syndrome: a case–control study evaluating its relationship with body mass index and hand and wrist measurements. J. Hand Surgery (Eur. Vol.) 33 (4), 445–448.
Filius, A., Scheltens, M., Bosch, H.G., Van Doorn, P.A., Stam, H.J., Hovius, S.E., Selles, R. W., 2015a. Multidimensional ultrasound imaging of the wrist: changes of shape and displacement of the median nerve and tendons in carpal tunnel syndrome. J. Orthop. Res. 33 (9), 1332–1340.
Filius, A., Thoreson, A.R., Wang, Y., Passe, S.M., Zhao, C., An, K.N., Amadio, P.C., 2015b. The effect of tendon excursion velocity on longitudinal median nerve displacement: differences between carpal tunnel syndrome patients and controls. J. Orthop. Res. 33 (4), 483–487.
Fleiss, J.L., 2011. Design and Analysis of Clinical Experiments. John Wiley & Sons.
Fowler, J.R., Gaughan, J.P., Ilyas, A.M., 2011. The sensitivity and specificity of ultrasound for the diagnosis of carpal tunnel syndrome: a meta-analysis. Clin. Orthop. Related Res.® 469 (4), 1089–1094.
Fröberg, Å., Cissé, A.-S., Larsson, M., Mårtensson, M., Peolsson, M., Movin, T., Arndt, A., 2017. Altered patterns of displacement within the Achilles tendon following surgical repair. Knee Surg. Sports Traumatol. Arthrosc. 25 (6), 1857–1865.
Gijsbertse, K., Goselink, R., Lassche, S., Nillesen, M., Sprengers, A., Verdonschot, N., De Korte, C., 2017. Ultrasound imaging of muscle contraction of the tibialis anterior in patients with facioscapulohumeral dystrophy. Ultrasound Med. Biol. 43 (11), 2537–2545.
Koo, T.K., Li, M.Y., 2016. A guideline of selecting and reporting intraclass correlation coefficients for reliability research. J. Chiropractic Med. 15 (2), 155–163.
Korstanje, J.-W.H., Selles, R.W., Stam, H.J., Hovius, S.E., Bosch, J.G., 2010. Development and validation of ultrasound speckle tracking to quantify tendon displacement. J. Biomech. 43 (7), 1373–1379.
Korstanje, J.W.H., Boer, M.S.D., Blok, J.H., Amadio, P.C., Hovius, S.E., Stam, H.J., Selles, R.W., 2012. Ultrasonographic assessment of longitudinal median nerve and hand flexor tendon dynamics in carpal tunnel syndrome. Muscle Nerve 45 (5), 721–729.
Lee, S.S., Lewis, G.S., Piazza, S.J., 2008. An algorithm for automated analysis of ultrasound images to measure tendon excursion in vivo. J. Appl. Biomech. 24 (1), 75–82.
Mondelli, M., Curti, S., Farioli, A., Aretini, A., Ginanneschi, F., Greco, G., Mattioli, S., 2015. Anthropometric measurements as a screening test for carpal tunnel syndrome: receiver operating characteristic curves and accuracy. Arthritis Care Research 67 (5), 691–700.
Nakamichi, K.I., Tachibana, S., 2000. Enlarged median nerve in idiopathic carpal tunnel syndrome. Muscle Nerve: Off. J. Am. Assoc. Electrodiag. Med. 23 (11), 1713–1718.
Shapiro, S.S., Wilk, M.B., 1965. An analysis of variance test for normality (complete samples). Biometrika 52 (3/4), 591–611.
Slane, L.C., Bogaerts, S., Thelen, D.G., Scheys, L., 2018. Nonuniform deformation of the patellar tendon during passive knee flexion. J. Appl. Biomech. 34 (1), 14–22.
Slane, L.C., Thelen, D.G., 2015. Achilles tendon displacement patterns during passive stretch and eccentric loading are altered in middle-aged adults. Med. Eng. Phys. 37 (7), 712–716.
Soeters, J.N., Roebroeck, M.E., Holland, W.P., Hovius, S.E., Stam, H.J., 2004a. Non-invasive measurement of tendon excursion with a colour Doppler imaging system: a reliability study in healthy subjects. Scand. J. Plast. Reconstr. Surg. Hand Surg. 38 (6), 356–360.
Soeters, J.N., Roebroeck, M.E., Holland, W.P., Hovius, S.E., Stam, H.J., 2004b. Reliability of tendon excursion measurements in patients using a color Doppler imaging system1. J. Hand Surg. 29 (4), 581–586.
Stegman, K.J., Djurickovic, S., Dechev, N., 2014. In vivo estimation of flexor digitorum superficialis tendon displacement with speckle tracking on 2-D ultrasound images using Laplacian, Gaussian and Rayleigh techniques. Ultrasound Med. Biol. 40 (3), 568–582.
van Beek, N., Gijsbertse, K., Selles, R.W., de Korte, C.L., Veeger, D.H., Stegeman, D.F., Maas, H., 2018. Tendon displacements during voluntary and involuntary finger movements. J. Biomech. 67, 62–68.
Van Doesburg, M.H., Yoshii, Y., Henderson, J., Villarraga, H.R., Moran, S.L., Amadio, P. C., 2012. Speckle-tracking sonographic assessment of longitudinal motion of the flexor tendon and subsynovial tissue in carpal tunnel syndrome. J. Ultrasound Med. 31 (7), 1091–1098.
Wiesler, E.R., Chloros, G.D., Cartwright, M.S., Smith, B.P., Rushing, J., Walker, F.O., 2006. The use of diagnostic ultrasound in carpal tunnel syndrome. J. Hand Surg. 31 (5), 726–732.
Witt, J.C., Hentz, J.G., Stevens, J.C., 2004. Carpal tunnel syndrome with normal nerve conduction studies. Muscle Nerve 29 (4), 515–522.
Yoshii, Y., Villarraga, H.R., Henderson, J., Zhao, C., An, K.-N., Amadio, P.C., 2009. Speckle tracking ultrasound for assessment of the relative motion of flexor tendon and subsynovial connective tissue in the human carpal tunnel. Ultrasound Med. Biol. 35 (12), 1973–1981.